

**Micromechanical properties of poly(butylene terephthalate) nanocomposites  
with single- and multi-walled carbon nanotubes**

**F. Ania<sup>1</sup>, G. Broza<sup>2</sup>, M.F. Mina<sup>3</sup>, K. Schulte<sup>2</sup>, Z. Roslaniec<sup>4</sup> and F.J. Baltá-Calleja<sup>1</sup>**

<sup>1</sup> Instituto de Estructura de la Materia, CSIC, Serrano 119, 28006-Madrid, Spain.

<sup>2</sup> Technical University of Hamburg-Harburg, Polymer Composites Section, Denickerstrasse 15,  
D-21071 Hamburg, Germany.

<sup>3</sup> Neutron Scattering Division, INST AERE, Dhaka, Bangladesh.

<sup>4</sup> Szczecin University of Technology, Institute of Materials Science and Engineering, Al. Piastów  
19, 70-310 Szczecin, Poland.

paper submitted to Composite Interfaces

revision: May 2005

Short title: Micromechanical properties of PBT/CNT composites

Correspondence to: F.J. Baltá Calleja (e-mail: [embalta@iem.cfmac.csic.es](mailto:embalta@iem.cfmac.csic.es))

## **ABSTRACT**

Polymer nanocomposites with carbon nanotubes (CNT) are becoming important structural materials because of their superior mechanical properties and easy processability. The objective of the work is to investigate the influence of small amounts of single walled carbon nanotubes (SWCNT), as well as multi-walled carbon nanotubes (MWCNT), on the microhardness of a thermoplastic polymer such as poly(butylene terephthalate) (PBT). The nanocomposites were obtained by introducing the CNT into the reaction mixture during the synthesis of PBT. The polymers without carbon nanotubes (reference material) and with carbon nanotubes were synthesized using an in-situ polycondensation reaction process. Weight percentages ranging from 0.01 to 0.2 wt% of the single walled and from 0.01 to 0.35 wt% of the multi-walled nanotubes were dispersed in 1,4-butanediol (BD) by ultrasonication and by ultrahigh speed stirring. The nanocomposites were extruded followed by injection molding. The samples were characterized by electron microscopy and microindentation hardness techniques. The variations of the micromechanical properties (indentation hardness) of the nanocomposites with nanotube content and with temperature are discussed in the light of the stress transfer between the polymer matrix and nanotubes, the degree of dispersion, the nature of the tubes and other structural parameters.

## **Keywords**

Poly(butylene terephthalate), carbon nanotube, composite, microhardness, in-situ polycondensation process, electron microscopy.

## 1 INTRODUCTION

Presently there is a wide choice of nanoscaled inorganic materials, such as carbon nanotubes (CNT), carbon nanofibrils, fullerenes or clay minerals that can be mixed with polymers. Among them, CNT have emerged as potentially ideal reinforcement for producing nanocomposites with unique physical properties [1-4]. Nanotubes have a large aspect ratio ( $>1000$ ), high Young's modulus, and low density and additionally they are short enough to allow mouldings of complex shapes [5-7]. For the above reasons, reports on the mechanical properties of polymer/CNT composites have considerably increased in the last five years [8-14]. The structure of CNT can be single-walled or multi-walled, the latter simply being composed of concentric single-walled nanotubes. The diameter of single-walled carbon nanotubes ranges from one up to a few nanometers, and their length is of a few  $\mu\text{m}$ . The small size of the nanotubes ensures a good surface finish, the high aspect ratio allows electrical percolation at very low loading, and the crystalline quality of the carbon results in a high conductivity and excellent mechanical properties as compared with the conventional carbon black [15,16]. Carbon nanotubes could be useful as well to modify a variety of matrix resins with respect to temperature and solvent resistance, crystallinity, nanostructure, thermal expansion coefficient, dielectric constant, and so on [7,15]. Despite these promises, difficulties have been encountered to exploit these impressive fundamental properties in real-life composites due to the need of dispersing the individual nanotubes within the matrix, and to ensure sufficient interfacial stress transfer between nanotubes and matrix [16]. On the other hand, the outstanding mechanical properties of CNT are of little value unless they can be successfully incorporated into a matrix.

In preceding studies we examined the influence of the incorporation of carbon fibers and fullerenes on the micromechanical properties of polymer composites [17,18]. The aim of the present study is to examine the effect of nanotube content and the influence of temperature on the micromechanical

properties (as derived from indentation experiments) of composites of poly(butylene terephthalate) (PBT) with small amounts of single- and multi-walled carbon nanotubes.

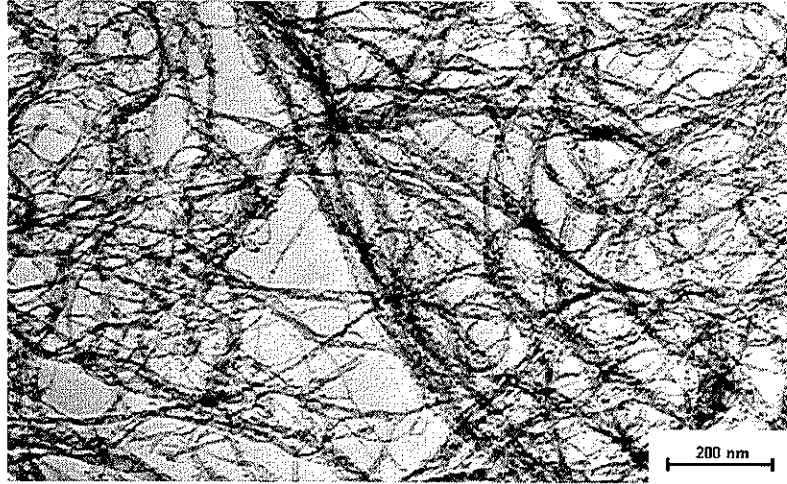


**Figure 1:** TEM image of single-walled carbon nanotubes.

## **2 EXPERIMENTAL**

### **2.1 Materials**

The reagents were purchased from BASF, Germany (1,4-butanediol) and DuPont, USA (dimethyl terephthalate). The oxidized single walled carbon nanotubes used in this study were kindly supplied by CNI Technology Co., Texas, USA [19], and have been synthesized by using the high-pressure conversion of carbon monoxide method (HiPCO method) [20]. The diameter of the tubes is in the range of 0.7-5 nm and their length is of a few  $\mu\text{m}$ . A TEM image of the SWCNT is presented in Fig. 1. Multi walled carbon nanotubes were produced in a Kratschmer-Hoffman generator at the Technical University of Hamburg-Harburg. The MWCNT have external diameters in the 5-20 nm range and lengths between 0.5 and 5  $\mu\text{m}$ . A TEM image of MWCNT is presented in Fig. 2.

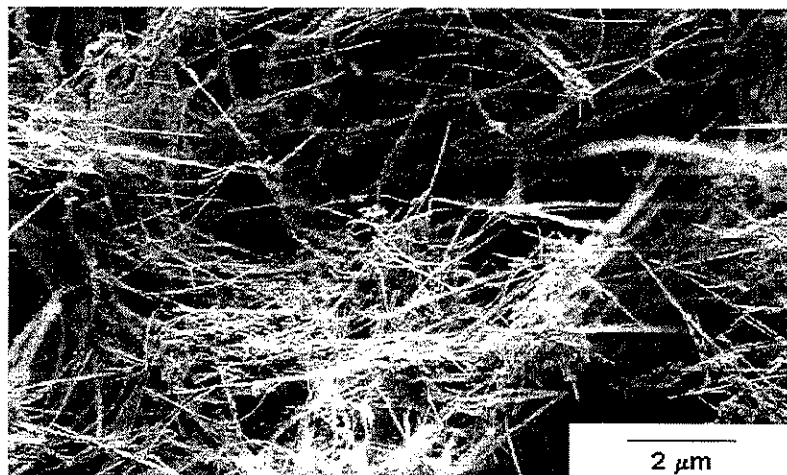


**Figure 2:** TEM image of multi-walled carbon nanotubes.

## **2.2 Processing of PBT/CNT nanocomposites**

Nanocomposites were obtained by introducing the nanotubes into the reaction mixture during the synthesis process of PBT by the polycondensation method in the molten state. Weight percentages ranging from 0.01 to 0.2 wt% of single walled and 0.01 to 0.35 wt% of multi-walled nanotubes were dispersed in 1,4-butanediol (BD) by ultrasonication applying a SONOPULS homogenizer HD2200 (equipped with a titanium tip sounder) from BANDELIN ELEKTRONIK GmbH, Berlin, Germany. The synthesis of PBT was a two-stage process carried out in an acid resistant steel reactor equipped with a controlled heating system, dephlegmator, horseshoe stirrer system with perpetual torque measurement, controlling system of the protective atmosphere and vacuum. During the first stage the process of transesterification of di(methyl terephthalate) (DMT) with BD proceeded at atmospheric pressure. The reaction was carried out in the temperature range of 150–190°C up to 90% reaction progress. The second stage was the polycondensation of a di(2-hydroxytetramethylene terephthalate) based mixture. The polycondensation was carried out in the 190–255°C range while decreasing the pressure gradually down to 10 Pa. The reaction progress was

estimated on the basis of the amount of distilled BD and the increase in the torque of the stirrer. The polymer was extruded out of the reactor by compressed nitrogen and pelletised. The molecular weight of the PBT composites was derived from their limiting viscosity number. The nanocomposites were dissolved in phenol-trichloroethylene 50:50 vol (0.5 wt%) and filtered by a poly(tetrafluoroethylene) (PTFE) membrane. The viscosity was measured in an Ubbelohde viscosimeter at 30°C and corrected by the weight of the polymer. Results show that the viscosity clearly decreases with increasing percent of CNT within the composite (from 0.97 dL/g for pure PBT down to 0.90 for 0.2% SWCNT and 0.74 dL/g for 0.5% MWCNT), suggesting a lower molecular weight for the nanocomposites than for the PBT reference material.

### 2.3 Techniques

The nanocomposites were first extruded and then tensile bars for mechanical testing were prepared by injection moulding using a Baby Plast injection moulding machine Model 6/10 (Cronoplast S.L. Comp.). Due to the very small amount of available raw material, a special processing machine with very low injection mass was used. The processing conditions were the same for the different nanocomposites. Tensile bars of non-reinforced PBT were similarly produced. Additionally, samples for transmission and scanning electron microscopy were cut from the tensile bars.

The morphology of the fractured surface of the injection-moulded samples was investigated using a field emission scanning electron microscope (SEM-FEG) model LEO 1530 (Leo Electron Microscopy Ltd., Zeiss, Oberhochem, Germany) after having applied a gold layer by means of a sputter coater. Ultra thin cuts were made with a diamond knife on a Leica Ultracut-E microtome. The thickness of the sections was about 60 nm. TEM elastic bright field images were taken on a Philips EM-402, operating at 100 kV.

A Vickers (Vickers Ltd., England) square-based diamond indenter was employed to measure the microindentation hardness  $H$  from the residual impression on the sample surface after an

indentation time of 0.1 min. Loads of 98, 147, 245 and 490 mN were used to derive a load-independent value of  $H$  (MPa) that was estimated by the following equation:

$$H = K (P/d^2) \quad (1)$$

where  $d$  (mm) is the indentation diagonal,  $P$  (N) the applied load and  $K$  a geometric factor equal to 1.854. During measurements, 10 imprints were taken for each load and the  $H$  values for all samples were determined within an error of  $\pm 3$  %. Microhardness experiments measured as a function of time provide the creep behaviour of a material. The time-dependent part of the plastic deformation is known to follow an equation of the form:

$$H = H_0 t^{-k} \quad (2)$$

where  $H_0$  is the microhardness value measured at a reference time  $t_0$  (1 min) and  $k$  is the creep constant. A constant load of 147 mN was applied for the creep measurements, which was held for periods of time  $t$  in the range 0.1-1000 min. The same load with loading times  $t = 0.1-100$  min was used to observe the  $H$  variation as a function of temperature ( $T$ ) ranging from 30°C to 100°C. A hot stage that can be controlled between room temperature and 200°C was used in the experiment. From these measurements, the variation of  $k$  with  $T$  was evaluated. The actual temperature was calibrated after melting known standards on the samples surface.

Differential Scanning Calorimetry (DSC) measurements were performed using a Perkin-Elmer DSC-7 instrument at a heating speed of 20 degrees per minute. Scans were calibrated in temperature and normalized according to sample weight.

### 3 RESULTS

#### 3.1 Morphology

A cryogenic fractured surface of PBT/CNT nanocomposites prepared with SWCNT is illustrated in the SEM micrograph of Fig. 3. The image shows a uniform nanotube distribution within the matrix. A significant amount of tubes pullout can also be observed. The presence of nanotube agglomerates

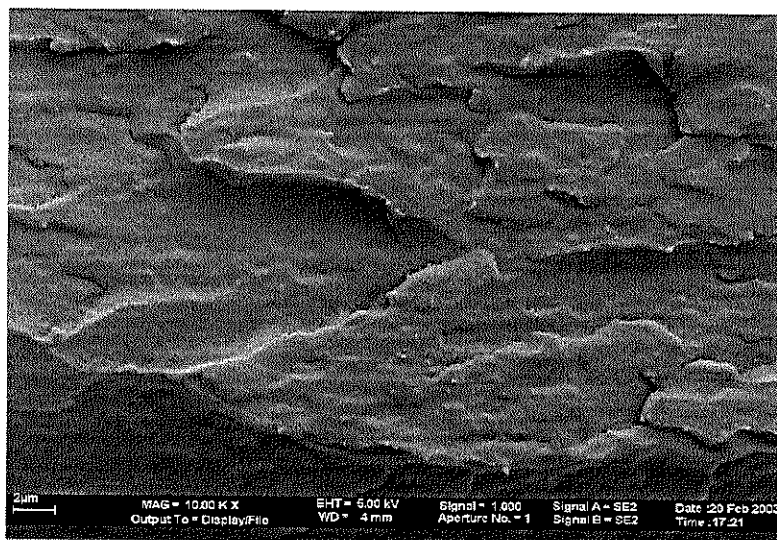


**Figure 3:** SEM micrograph of the cryogenic fractured surface of a PBT/CNT sample containing 0.1 wt% SWCNT.

in the matrix could not be so far identified. The dispersion of CNT in the BD may wrap these tubes to prevent their aggregation upon the evaporation surplus of BD during the polycondensation reaction. SEM micrographs permit to distinguish individual MWCNT in these composites [Fig. 4].

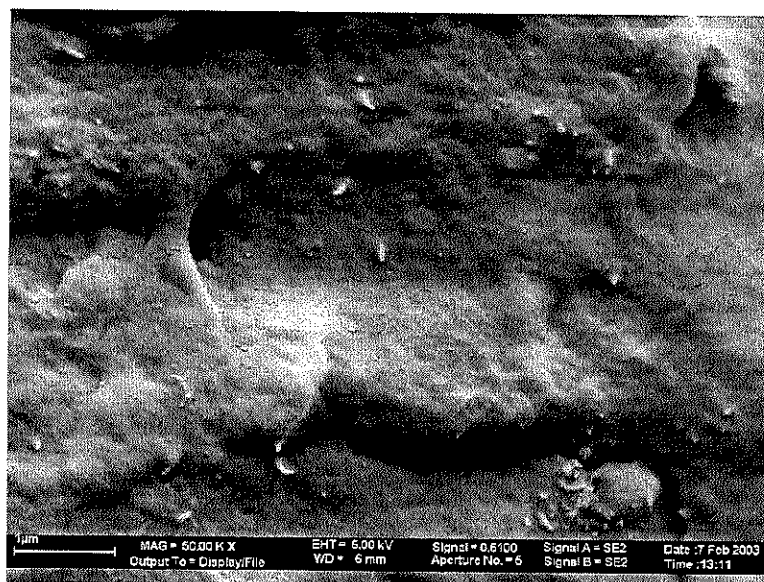


**Figure 4:** SEM micrograph of the cryogenic fractured surface of a PBT/CNT sample containing 0.2 wt% MWCNT.



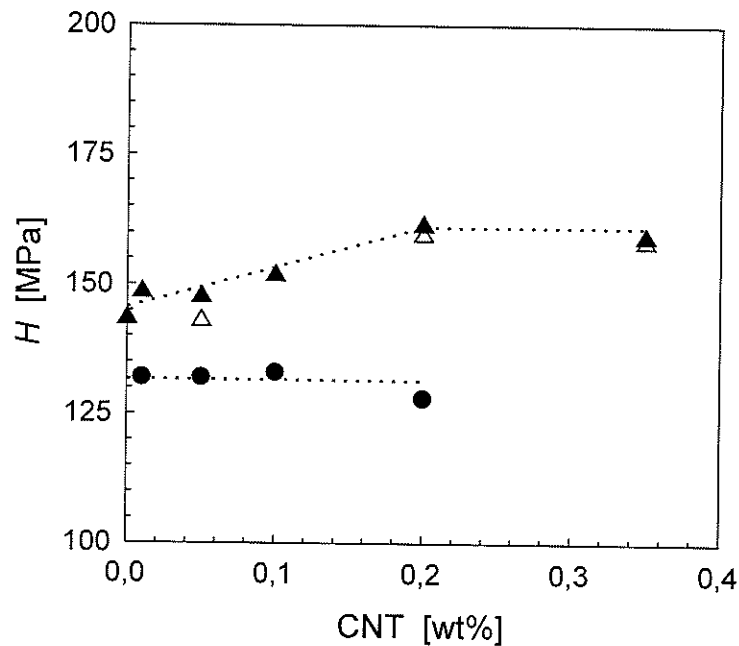


**Figure 5:** Microhardness  $H$  of PBT/CNT composites as a function of wt% CNT. (●: SWCNT; ▲: MWCNT; △: MWCNT composites with  $\text{NH}_2$  groups at the surface).

### 3.2 Microhardness Data

The microhardness of the PBT/CNT composites as a function of percent weight of carbon nanotubes is shown in Fig. 5. Despite the limited number of filler contents available, in case of the MWCNT composites, it is observed that  $H$  increases from a value of 143 MPa for the pure PBT up to about 160 MPa for a 0.2% of carbon nanotubes. For a higher concentration of MWCNT (0.35%) a levelling-off  $H$  value is obtained. The microhardness data of the materials containing  $\text{NH}_2$  groups at the surface do not significantly differ from those of untreated MWCNT. It means that, in this case, the surface modification does not seem to modify the micromechanical properties. The hardness behaviour observed in case of SWCNT composites is somewhat different: 1) the composites show lower microhardness values than the preceding ones and 2) the addition of CNT yields  $H$  values which are practically constant for the concentration range studied. It is to be noted that the sample with 0.2% CNT shows a slightly lower  $H$  value.

When using a different polymer matrix, on the PBT basis, such as the polyester-ether block copolymer PBT/poly(tetramethylene oxide) (PTMO) with 45 wt% of hard segments, and 55 wt% of soft segments, the addition of small proportions of MWCNT or SWCNT also induces negligible changes on the  $H$  values of the composite (Fig. 6).

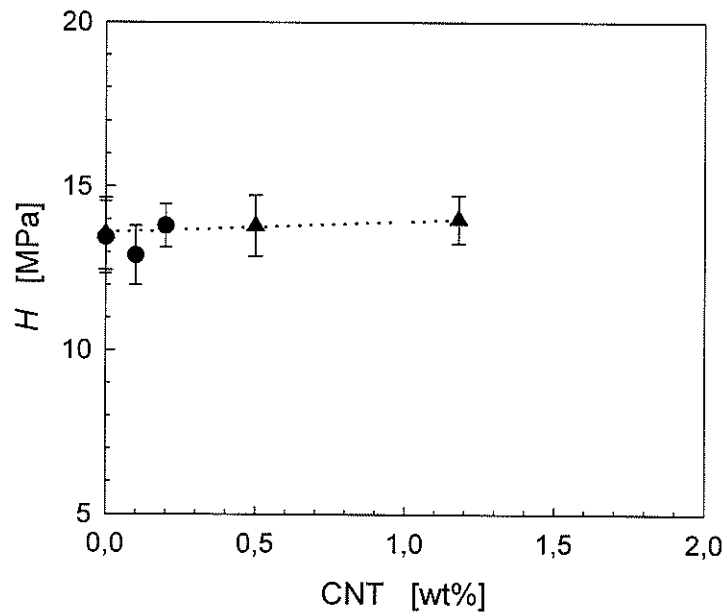


**Figure 6:** Microhardness  $H$  of PBT/PTMO/CNT composites as a function of wt% CNT. (●: SWCNT; ▲: MWCNT).

By plotting the microhardness value of the PBT/SWCNT composites as a function of indentation time in a log-log plot (see eq. 2), one can derive the creep constant,  $k$  of each material from the slope of the decreasing linear variation of  $\log H$  vs.  $\log T$ . Fig. 7 shows the variation of the creep constant  $k$  as a function of SWCNT concentration of the above-mentioned composites. According to the usual trend, the  $k$  values present an opposite behaviour as those of  $H$ : i.e. an initial  $k$  decrease, followed by a levelling-off for the highest CNT content.

Let us next examine the variation of  $H$  with temperature for the PBT/SWCNT composites studied. Fig. 8 illustrates the microhardness values corresponding to the different compositions, starting with the pure polymer. The different curves are shifted vertically for the sake of clarity. In all cases,

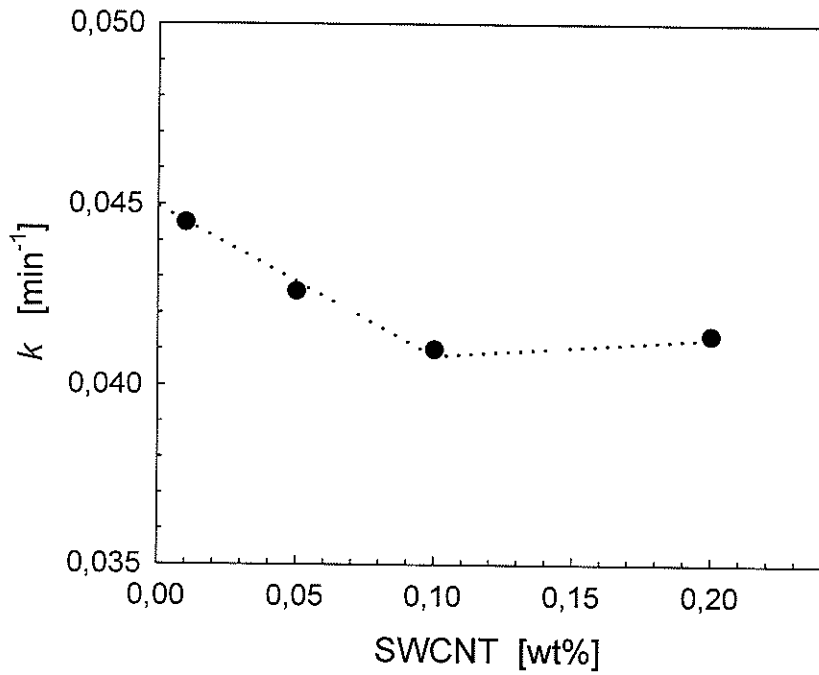


**Figure 7:** Creep constant derived from microhardness measurements as a function of wt% SWCNT.

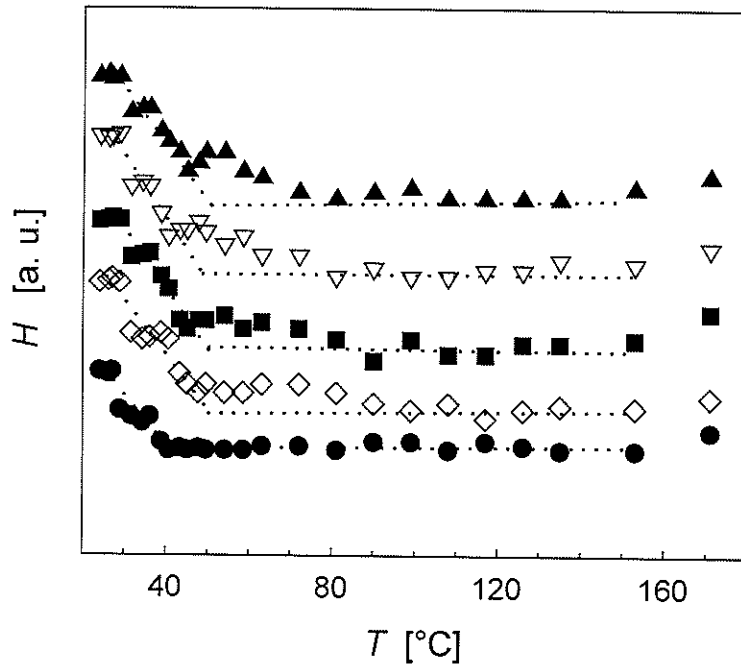


**Figure 8:** Temperature dependence of  $H$  for the PBT/SWCNT composites. (●: PBT; ◇: PBT/0.01 wt% SWCNT; ■: PBT/0.05 wt% SWCNT; ▽: PBT/0.1 wt% SWCNT; ▲: PBT/0.2 wt% SWCNT).

$H$  shows an initial clear step decrease, followed by a broad plateau at intermediate temperatures (40-150°C), which seems to end with a slight  $H$  increase at higher temperatures. The intercept between the initial linear decrease and the horizontal plateau, defines a temperature that should be close related to the glass transition temperature of each sample [21]. Such temperature is of around 40°C for the pure polymer matrix and increases up to about 50°C for the rest of the composites. It is to be noted that the bend in the  $H$ - $T$  plots occurs at temperatures slightly lower than the usual reported  $T_g$  value of the PBT matrix. For the composite materials there is an additional  $H$  increase, in the form of broad shoulder, immediately above 50°C. Such a microhardness peak with temperature becomes narrower with increasing SWCNT concentration and somehow resembles the positive  $H$  dependence found for polyethylene-fullerene composites above 75°C, which was tentatively associated to a rearrangement of  $C_{60}$  aggregates within the composite [18].

Fig. 9 depicts the temperature cycle of the first and second heating curves and the final cooling for the PBT/0.01% SWCNT. One clearly observes that during the first heating process an irreversible

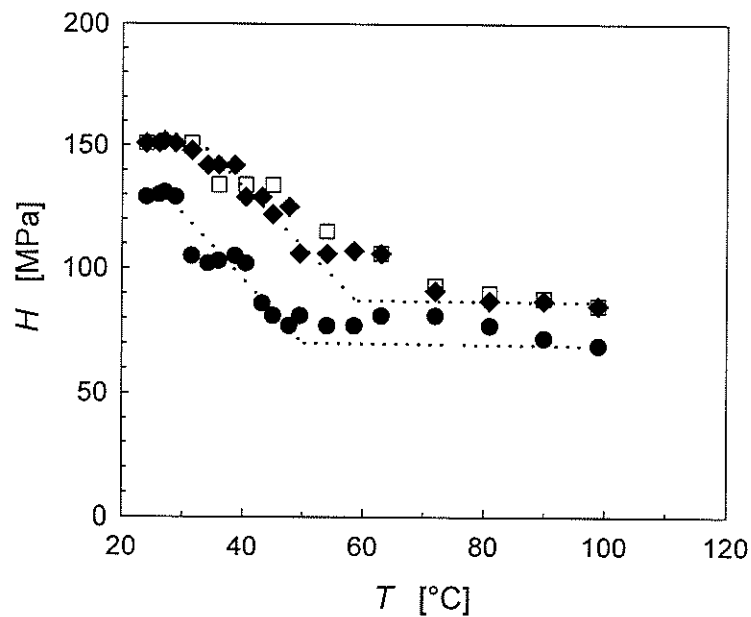


**Figure 9:** Variation of  $H$  during various temperature cycles for PBT/0.01 wt% SWCNT. (●: first heating run; ◆: second heating; □: cooling after 2<sup>nd</sup> heating run).

microhardness increase, together with a 10°C shift of the transition temperature towards higher temperatures, takes place. This shift permits to define more accurately the temperature interval close to room temperature, which occurs prior to the above mentioned stepwise decrease.

#### 4 DISCUSSION

In spite of recent experimental and theoretical results confirming the excellent mechanical properties of individual carbon nanotubes (as high as 1 TPa for the tensile modulus [22-24]), it is evident that this value cannot be directly used to estimate the mechanical properties of polymer/CNT composites due to the defective stress transfer between the matrix and the tubes and the discontinuous stress transfer inside the nanotubes [25]. Another important issue regarding the micro-mechanics of composites is the large degree of dispersion of the reinforcement material inside the polymer matrix. According to our SEM micrographs (Fig. 3 and Fig. 4), the introduction of the nanotubes into the reaction mixture during the synthesis of PBT yields a quite uniform distribution of the nanotubes. However the adhesion between the tubes and the matrix is apparently poor, as suggested by the significant pullout observed in the fracture surfaces (Fig. 3 and Fig. 4). The chemical functionalization of carbon nanotubes has been lately proposed as a way to improve the mechanical load transfer to the polymer matrix through chemical bonds, as well as to ensure homogeneous nanotube dispersion [26,27].

The correlation between microhardness,  $H$ , and tensile modulus,  $E$ , as derived from tensile experiments in case of polyethylene is found to follow Struik's relation  $H \sim 10 / E$  [28]. From this relationship and from the above mentioned tensile modulus value of pure carbon nanotubes, a rough estimation for the microhardness of the latter of about 100 GPa can be made. It is clear that neither our measurements, nor the few previously reported microhardness data on polymer/CNT composites [9,10,12] approach by far the values arising from a simple rule of mixing derived from

the above estimation. The best results for non-functionalized CNT composites have been obtained so far for nylon 6 (PA6)/MWCNT composites which, with the incorporation of 2 wt% MWCNT, show a 210% and a 80% increase in tensile modulus and microhardness, respectively, as compared with neat PA6 [12]. In our case, the addition of 0.2 wt% MWCNT to PBT yields a 12% increase in  $H$  (Fig. 5). On the contrary, the same amount of SWCNT in the same polymer matrix does not produce any significant effect on the surface mechanical properties of the composite. At this point, it is not yet clear which is the origin of such a different behaviour. A general trend in the investigation of the mechanical properties of this type of composites seems to be the wide variety of data obtained, which immediately leads to the conclusion that many different factors should be contributing to the final results. Only in this work, the selection of a different polymer matrix, such as PBT/PTMO, makes that both MWCNT and SWCNT fillers do not contribute to any  $H$  increase of the composites (Fig. 6).

In addition to the varying CNT-matrix adhesion and the different dispersion of the nanotubes, the crystallization of the polymer matrix may experience quite different behaviours due to the presence of nanotubes. It has been reported that the half time of crystallization may increase together with an increase in the crystallization rate, which in some cases also leads toward a higher total degree of crystallinity [29]. For polypropylene mixed with carbon nanotubes, it has been even found the appearance of a different crystal modification [30].

It has also been shown that the glass transition temperature of a number of polymer/CNT composites increasing with filler content [31,32]. In our case, a 10°C increase of  $T_g$  can be estimated from the comparison of the temperature variation of the microhardness for pure PBT and different SWCNT composites, as shown in Fig. 8. The shift of  $T_g$  to higher temperatures is generally associated with the appearance of a rigid amorphous phase [33]. Such a temperature change could be due to the fact that some polymer chain segments in the amorphous phase are restricted to move between crystalline regions, which act as fixation points. The temperature cycles

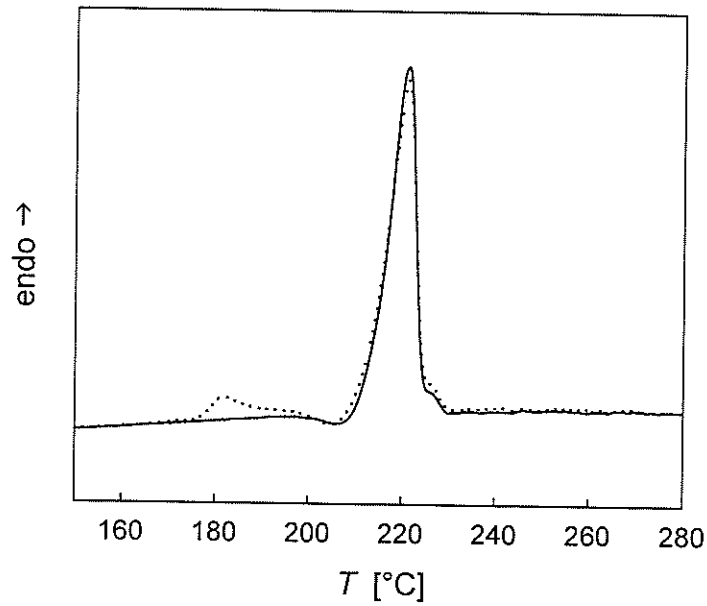


**Figure 10:** DSC thermograms of PBT/0.01 wt% SWCNT: before (continuous line) and after annealing at 175°C for one hour (dotted line).

depicted in Fig. 9 for a PBT/0.01 wt% SWCNT composite show, after the first heating cycle, a permanent  $H$  increase at all temperatures, together with a shift of  $T_g$  towards higher temperatures. Both phenomena should be related to a crystallinity increase of the material occurring at temperatures above  $T_g$ . In order to verify the latter contention, DSC thermograms for a composite with 0.01% SWCNT, before and after annealing at 175°C during 1 h, were performed. This annealing process attempts to reproduce the thermal treatment of the samples in Fig. 9 during the microhardness measurements. Results in Fig. 10 reveal that both samples exhibit a similar melting peak at 221°C [34]. The annealed composite shows, in addition, a second broad melting peak in the DSC scan at temperatures slightly higher than the annealing temperature. The presence of multiple endothermic peaks is well known for PBT and many other polyesters [35]. The low-temperature endotherm can be assigned to the melting of smaller crystallites, which were formed at the annealing temperature and which consequently increase the initial crystallinity index. Such an

increase of crystallinity (~8%) may provoke indeed the observed shift of the microhardness values during the second temperature cycle.

A final issue, which should be taken into consideration, is the possible orientation of the nanotubes that could play an important role in the overall mechanical properties. In the case of microindentation hardness, even small areas of local orientation could contribute to obtain quite different results. However, in our case a series of  $H$  measurements along the cross-section of the outer surface and of the central area of the samples has ruled out the existence of any indentation anisotropy.

## 5 CONCLUSIONS

1. The addition of up to 0.2 wt% MWCNT to PBT induces an increase of the microhardness of about 12 %. The  $H$  values obtained are much smaller than those derived from the elastic modulus using Struik's relation. The use of SWCNT does not improve the micromechanical properties.
2. It is shown that the time dependent part of the plastic deformation (creep constant) under the indenter diminishes appreciably with increasing SWCNT content, in contrast with the usual slight decrease found in other common polymer materials.
3. The temperature dependence of  $H$  for the SWCNT composites shows a clear decrease below  $T_g$  followed by a levelling-off of the hardness value at higher temperatures.
4. The study of the  $H$  variation during various temperature cycles for PBT/0.01 wt% SWCNT composites shows an irreversible  $H$  increase (hysteresis) during the first cycle together with a shift of  $T_g$  towards higher temperatures. Both phenomena can be related to the crystallinity increase that takes place in the PBT matrix during annealing.



## ACKNOWLEDGEMENTS

F.A. and F.J.B.C. acknowledge the Ministerio de Educación y Ciencia (Grant No. FIS2004-01331), Spain, for the generous support of this investigation. M.F.M. thanks the Secretaría de Estado de Educación y Universidades del Ministerio de Educación, Spain, for the award of a grant (Ref. SB2000-0478). G.B., K.S. and Z.R. gratefully acknowledge the European Commission (Scientific Network: "Carbon Nanotubes for Future Industrial Composites: theoretical potential versus immediate application (CNT-Net)"; Contract N°: G5RT-CT-2001-050206) for financial support.

## REFERENCES

1. X. Liu, Q. Wu, L.A. Berglund, J. Fan and Z. Qi, *Polymer*, 42(19), 8235 (2001)
2. Z. Jin, K.P. Pramoda, G. Xu and S.H. Goh, *Chem. Phys. Lett.*, 337, 43 (2001)
3. J. Sandler, M.S.P. Shaffer, T. Prasse, W. Bauhofer, K. Schulte and A.H. Windle, *Polymer*, 40, 5967 (1999)
4. Ch.I. Park, O.Ok. Park, J.G. Lim and H.J. Kim, *Polymer*, 42(17), 7465 (2001)
5. P. Calvert, *Nature*, 399, 210, May (1999)
6. J.P. Salvetat, G.A.D. Briggs, J.M. Bonard, R.R. Bacsá, A.J. Kulik, T. Ströckli, N.A. Burnham and L. Forró, *Phys. Rev. Lett.*, 82(5), 944 (1999)
7. S. Subramoney, *Adv. Mater.*, 10(15), 1157 (1998)
8. Z. Jin, K.P. Pramoda, G. Xu and S.H. Goh, *Chem. Phys. Lett.*, 337, 43 (2001)
9. C.A. Cooper, D. Ravich, D. Lips, J. Mayer and H.D. Wagner, *Composites Sci. and Technol.*, 62, 1105 (2002)
10. W. Tang, M.H. Santare and S.G. Advani, *Carbon*, 41, 2779 (2003)
11. Z. Roslaniec, G. Broza and K. Schulte, *Composite Interfaces*, 10, 95 (2003)
12. T. Liu, I.Y. Phang, L. Shen, S.Y. Chow and W-D. Zhang, *Macromolecules*, 37, 7214 (2004)
13. R.E. Gorga and R.E. Cohen, *J. Polym. Sci. Part B - Polymer Phys.*, 42, 2690 (2004)

14. L.M. Clayton, T.G. Gerasimov, M. Cinke, M. Meyyappan and J.P. Harmon, *Polymer Bulletin*, 52, 259 (2004)
15. X. Gong, J. Liu, S. Baskaran, R.D. Voise and J.S. Young, *Chem. Mater.*, 12, 1049 (2000)
16. A.H. Barber, S.R. Cohen and H.D. Wagner, *Appl. Phys. Lett.*, 82(23), 4140 (2003)
17. W.P. Paplham, J.C. Seferis, F.J. Baltá Calleja and H.G. Zachmann, *Polymer Composites*, 16(5), 424 (1995)
18. F.J. Baltá Calleja, L. Giri, T. Asano, T. Mieno, A. Sakurai, M. Ohnuma and C. Sawatari, *J. Mater. Sci.*, 31, 5153 (1996)
19. Carbon Nanotechnologies Inc. (CNI), 16200 Park Row, Houston, TX 77084, USA
20. P. Nikolaev, M.J. Bronikowski, R.K. Bradley, F. Rohmund, D.T. Colbert, K.A. Smith and R.E. Smalley, *Chem. Phys. Lett.*, 313, 91 (1999)
21. F. Ania, J. Martínez-Salazar and F.J. Baltá Calleja, *J. Mater. Sci.*, 24, 2934 (1989)
22. O. Lourie, D.M. Cox and H.D. Wagner, *Phys. Rev. Lett.*, 81, 1638 (1998)
23. J.P. Salvetat, G.A.D. Briggs, J-M. Bonard, R.R. Bacsa, A.J. Kulik, T. Stöckli, N.A. Burnham and L. Forró, *Phys. Rev. Lett.*, 82, 944 (1999)
24. F. Li, H.M. Cheng, S. Bai, G. Su, M.S. Dresselhaus, *Appl. Phys. Lett.*, 77, 3161 (2000)
25. K-T. Lau, M. Chipara, H-Y. Ling and D. Hui, *Composites: Part B*, 35, 95 (2004)
26. C. Velasco-Santos, A.L. Martínez-Hernández, F.T. Fisher, R. Ruoff and V.M. Castano, *Chem. Mater.*, 15(23), 4470 (2003)
27. Y. Lin, B. Zhou, K.A. Shiral Fernando, P. Liu, L.F. Allard and Y-P. Sun, *Macromolecules*, 36, 7199 (2003)
28. L.C.E. Struik, *J. Noncryst. Solids*, 131-133, 395 (1991)
29. M. Cadek, J.N. Coleman, V. Barron, K. Hedicke and W.J. Blau, *Appl. Phys. Lett.*, 81(27), 5123 (2002)

30. L. Valentini, J. Biagiotti, J.M. Kenny and M.A.L. Manchado, *J. Appl. Polym. Sci.*, 89(10), 2657 (2003)
31. X. Gong, J. Liu, S. Baskaran, R.D. Voise and J.S. Young, *Chem. Mater.*, 12(4), 1049 (2000)
32. J.W. Yang, J.H. Hu, C.C. Wang, Y.J. Qin and Z.X. Guo, *Macromol. Mater. Eng.*, 289(9), 828 (2004)
33. B. Wunderlich, *Prog. Polym. Sci.*, 28, 383 (2003)
34. K-Ch. Chiou and F-Ch. Chang, *J. Polym. Sci: Part B, Polym. Phys.*, 38, 23 (2000)
35. P. Cebe and S. Chung, *Polym. Compos.*, 11, 265 (1990)